International Journal of
Molecular Sciences

MDPI

Article

Effects of Ultra-Weak Fractal Electromagnetic Signals on *Malassezia furfur*

Pierre Madl [1,2], Roberto Germano [3], Alberto Tedeschi [4] and Herbert Lettner [5,*]

[1] Department of Biosciences & Medical Biology, University of Salzburg, A-5020 Salzburg, Austria
[2] Prototyping Unit, Edge-Institute at ER-System Mechatronics, A-5440 Golling, Austria
[3] Edge-Institute Italia at PROMETE Srl, CNR Spin off, I-80125 Napoli, Italy
[4] Research & Development Unit, Edge-Institute Italia at WHB, I-20123 Milan, Italy
[5] Department of Chemistry and Physics of Materials, Laboratory of Environmental Biophysics, University of Salzburg, A-5020 Salzburg, Austria
* Correspondence: herbert.lettner@plus.ac.at

Abstract: *Malassezia* spp. are dimorphic, lipophilic fungi that are part of the normal human cutaneous commensal microbiome. However, under adverse conditions, these fungi can be involved in various cutaneous diseases. In this study, we analysed the effect of ultra-weak fractal electromagnetic (uwf-EMF) field exposure (12.6 nT covering 0.5 to 20 kHz) on the growth dynamics and invasiveness of *M. furfur*. The ability to modulate inflammation and innate immunity in normal human keratinocytes was also investigated. Using a microbiological assay, it was possible to demonstrate that, under the influence of uwf-EMF, the invasiveness of *M. furfur* was drastically reduced (d = 2.456, $p < 0.001$), while at the same time, its growth dynamic after 72 h having been in contact with HaCaT cells both without (d = 0.211, $p = 0.390$) and with (d = 0.118, $p = 0.438$) uwf-EM exposure, were hardly affected. Real-time PCR analysis demonstrated that a uwf-EMF exposure is able to modulate human-β-defensin-2 (hBD-2) in treated keratinocytes and at the same time reduce the expression of proinflammatory cytokines in human keratinocytes. The findings suggest that the underlying principle of action is hormetic in nature and that this method might be an adjunctive therapeutic tool to modulate the inflammatory properties of *Malassezia* in related cutaneous diseases. The underlying principle of action becomes understandable by means of quantum electrodynamics (QED). Given that living systems consist mainly of water and within the framework of QED, this water, as a biphasic system, provides the basis for electromagnetic coupling. The oscillatory properties of water dipoles modulated by weak electromagnetic stimuli not only affect biochemical processes, but also pave the way for a more general understanding of the observed nonthermal effects in biota.

Keywords: *Malassezia furfur*; HaCaT; FRACTOS; hormesis; fractal ULF/VLF stimulation; QED

Citation: Madl, P.; Germano, R.; Tedeschi, A.; Lettner, H. Effects of Ultra-Weak Fractal Electromagnetic Signals on *Malassezia furfur*. *Int. J. Mol. Sci.* **2023**, *24*, 4099. https://doi.org/10.3390/ijms24044099

Academic Editors: Nikolaj Sorgenfrei Blom, Pierre Madl and Livio Giuliani

Received: 6 December 2022
Revised: 30 January 2023
Accepted: 9 February 2023
Published: 17 February 2023

Copyright: © 2023 by the authors. Licensee MDPI, Basel, Switzerland. This article is an open access article distributed under the terms and conditions of the Creative Commons Attribution (CC BY) license (https://creativecommons.org/licenses/by/4.0/).

1. Introduction

Yeasts are single-celled eukaryotic microorganisms. Taxonomically, *Malassezia furfur* is grouped under the subkingdom Dikarya, division Basidomycota, order Malasseziales [1]. The genus *Malassezia* comprises lipophilic fungal species whose natural habitat is the skin of humans and other warm-blooded animals [2]. However, *M. furfur* is not only commensal, but it can be involved in the pathogenesis of various dermatological diseases such as folliculitis, *Pityriasis versicolor*, dandruff, *Seborrheic dermatitis*, atopic dermatitis, and psoriasis in individuals with a genetic predisposition [3,4].

The skin, as a physical barrier, is impermeable to most pathogens and thus is the first line of defense. At the same time, it acts also as a chemical barrier by providing cytokines/chemokines, proteases, and antimicrobial peptides/proteins. Keratinocytes secrete a number of soluble factors that are capable of modulating an immune response

[5]. Interleukin-(IL)-8, a potent chemoattractant for neutrophils, has been shown to be expressed from keratinocytes in psoriasis and via the stimulation of other cytokines. IL-1β, IL-6, and tumor necrosis factor α (TNF-α) are also important chemical mediators, which are secreted by activated keratinocytes [6] in the acute inflammatory phase and during the healing process of skin lesions alike [7]. Hence, *Malassezia* species may act as controllers of innate immunity. Ishibashi et al. [8] found that *M. globosa* induced the expression of IL-6 in normal human epidermal keratinocytes (NHEKs), while Baroni et al. [9] showed that *M. furfur* upregulated the gene expression of IL-8 (along with toll-like receptor (TLR-2) and human-β-defensin-2 (hBD-2) when co-cultured with *M. furfur*.

Antimicrobial peptides of the hBD family are expressed in all human epithelial tissues as they represent an ancient branch of the innate immune system whose role is to promptly neutralize invading microbes [10]. Conventional therapeutic countermeasures for the treatment of diseases, such as *Malassezia folliculitis*, *Pityriasis versicolor*, dandruff, and *Seborrheic dermatitis,* rely on azoles (antifungal agents such as ketoconazole, itraconazole, fluconazole, etc.), which have an inhibitory effect against *Malassezia* species. Skin diseases associated with *Malassezia* species are chronic and recurrent disorders, requiring repeated therapy. Photodynamic inactivation (PDI), for example, is a novel and effective physicochemical therapeutic option [11]. It relies on two components—electromagnetic radiation in the visible range combined with a photosensitizer as an additive—to unfold the antimicrobial effect. While PDI operates already with low-dose photosensitiser concentrations, bio-electromagnetism can operate with even lower dosages, revealing a biphasic dose–response relationship [12], i.e., a low dose stimulation manifests itself as a beneficial effect, whereas it results in inhibitory effects when administered in high doses. Although ample literature has accumulated over past decades on the adverse effects of high-dose electromagnetic stimulation (see selected publications [13–21]), there are currently only a few studies available addressing the low-dose effect of electromagnetic stimulation ([22], and references therein)—for details see the Appendix. Given that hormetic effects per se are already difficult to perceive under the current biological paradigm, we feel there is a need to bridge the prevailing atomistic/molecular worldview with the field aspect initiated by Schrodinger [23]. Over the decades that followed, this branch of physics elaborated a respectable body of knowledge that no longer restricts itself to solid-state physics, but gradually makes its way into soft-matter physics, with quantum electrodynamics (QED) being the foremost promoter—for details we likewise ask the reader to consult the Appendix.

In this investigation, we utilize ultra-weak fractal electromagnetic (uwf-EM) signals that have already been used to stimulate biological samples [24–26]. This concept has recently been further refined using a revised prototype termed FRACTOS [26]. However, in doing so, we used an updated version of this prototype to investigate the response of HaCaT cells infected with *Malassezia furfur* by treating both with a uwf-EM signal. This device essentially consists of a logarithmic coil printed on a circuit board, connected to a signal source, which provides an audio signal (in the 0.5 to 20 kHz range) and whose loudness–frequency relation has fractal properties [27]. The logarithmic coil progression was chosen as it occurs in all domains of life and is expressed in the physiological and functional properties of living systems [28]. Thus, we demonstrate with this approach that such signals can indeed modulate the inflammatory response of infected HaCaT cells and enhance cytoprotective responses via hBD-2.

2. Results

2.1. Effect of uwf-EMF Treatment on Malassezia furfur Invasivity

Yeast cells plated on Sabouraud agar and treated with the uwf-EM signal showed a reduction in growth dynamics compared to untreated cells. As shown in Figure 1 (respectively, Table 1), a 35% reduction in *M. furfur* invasiveness was found after 72 h with respect to *M. furfur* batches for both HaCaT-exposed (effect size d = 2.456 with a

significance value $p < 0.001$) as well as HaCaT-unexposed cells (effect size d = 3.555 with a significance value $p = 0.018$). To determine whether *M. furfur* is capable of affecting the invasiveness of the yeast controls, HaCaT cultures were infected with uwf-EM pre- and untreated *M. furfur* cultures (at a 1:30 cell:yeast ratio). After 48 h, the effect of uwf-EM exposure on *M. furfur*'s invasiveness was assessed.

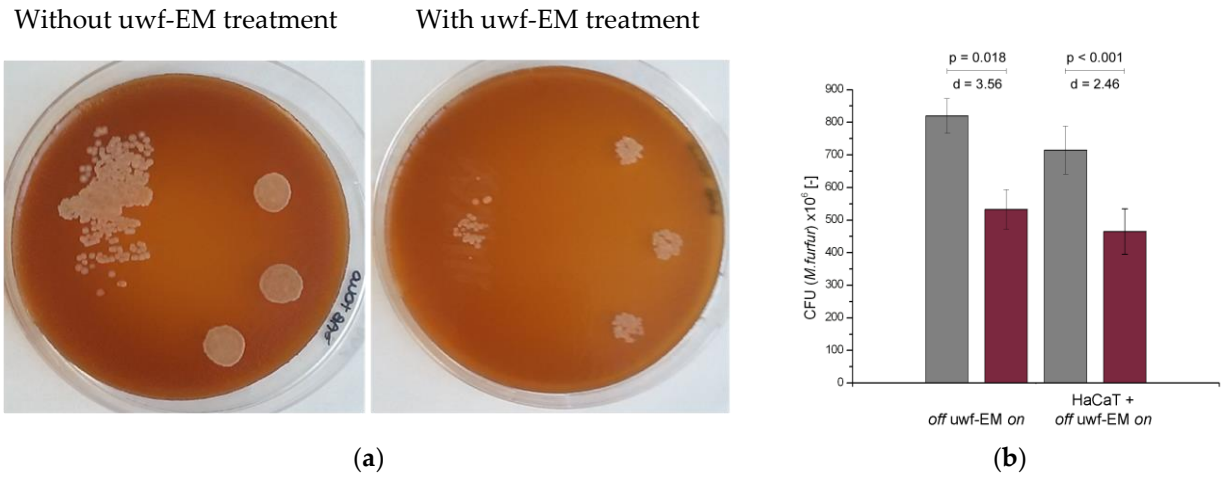

Figure 1. CFUs conducted on *M. furfur* in three replicates after 48 h of incubation (**a**) with (**right pane**) and without (**left pane**) uwf-EM pre-treatment. (**b**) Quantitative representation of CFU-counts of *M. furfur*. Colour codes: gray, without uwf-EM stimulation, red with uwf-EM stimulation. Both the calculated effect sizes (d) and *p*-values ($p < 0.05$) underline the statistical significance of the results.

Table 1. CFU counts of *M. furfur* following 48 h of incubation. Both emf-EM-exposed cultures (those in contact with and without HaCaT cells) show a 35% reduction in CFUs compared to non-uwf-EM-exposed controls.

48 h (CFU ×10⁶)	Trial 1	Trial 2	Trial 3	Average ± STDev
uwf-EM off	832	762	866	820 ± 53.0
uwf-EM on	466	584	550	533 ± 60.7
HaCaT + uwf-EM off	789	714	641	715 ± 74.0
HaCaT + uwf-EM on	534	467	395	465 ± 69.5

2.2. Effect of uwf-EM Signals on HaCaT Cells Exposed to Malassezia furfur

Human keratinocytes were cultured with or without *M. furfur* in a 30:1 ratio (yeast cells to keratinocytes). To monitor the cell proliferation of HaCaT cells, spectrometric absorbance measurements were performed every 24 h - shown in Figure 2 (respectively, Table 2). The corresponding optical density corresponds to the mass concentration of the HaCaT cells infected with or without *M. furfur* as well as with and without uwf-EM treatment. The steadily increasing absorbance with time (accumulation of formazan concentration within and on the cell surfaces) indicates that the mitochondrial reductase of the HaCaT cells maintained adequate vitality, even after 72 h of incubation. This implicates that uwf-EM treatment did not alter the viability of the cells.

Table 2. Numeric representation of CFUs versus time as averages of three replicates along with the corresponding standard deviations.

Time [h]	HaCaT Ctrl	HaCaT + *M. furfur*	HaCaT + *M. furfur* + uwf-EM
0	0.881 ± 0.026	0.848 ± 0.039	0.884 ± 0.009
24	1.071 ± 0.057	1.395 ± 0.016	1.307 ± 0.047
48	1.450 ± 0.040	1.595 ± 0.123	1.494 ± 0.047
72	1.670 ± 0.143	1.705 ± 0.088	1.643 ± 0.179

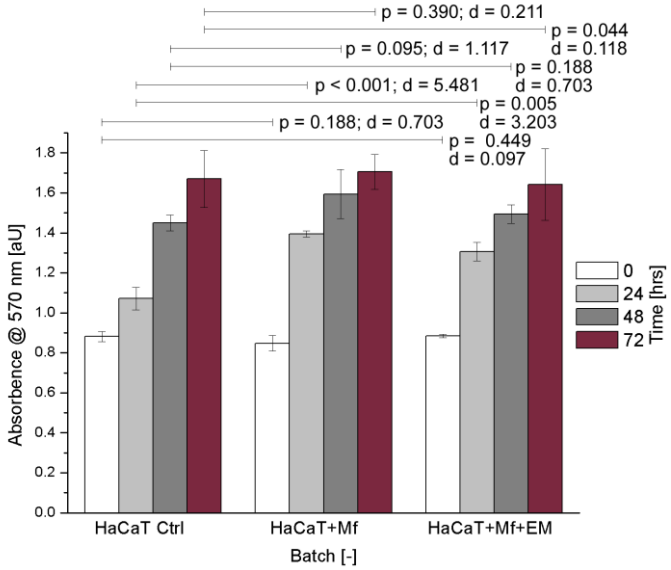

Figure 2. HaCaT cell cultures showing the control, *M. furfur*-infected, and *M. furfur*-infected cells that have been treated with the uwf-EM signal. Both the calculated effect sizes (d) and *p*-values ($p < 0.05$) highlight the inexistence of a statistically significant difference after 72 h with $p = 0.390$ vs. d = 0.211 for HaCaT + *M. furfur* exposure and $p = 0.044$ vs. d = 0.118 for HaCaT + *M. furfur* + uwf-EM exposure combined.

2.3. Effect of uwf-EM Signals on the Proinflammatory Response of HaCaT Cells Infected with Malassezia furfur

To investigate the potential of uwf-EM exposure to modulate the inflammatory response, we also evaluated gene the expression of cytokines in noninfected HaCaT cells as well as in infected ones with and without uwf-EM pre-treated *Malassezia*. As shown in Figure 3 (respectively, Table 3), we detected a marked increase in the IL-6, IL-8, and IL-1α gene expression in the HaCaT cells following an infection with *M. furfur* after 24 h of incubation; the infection boosted IL-6 and IL-1α by a factor of ≈3 compared to uninfected HaCaT cells, while IL-8 increased almost by a factor of ≈5.

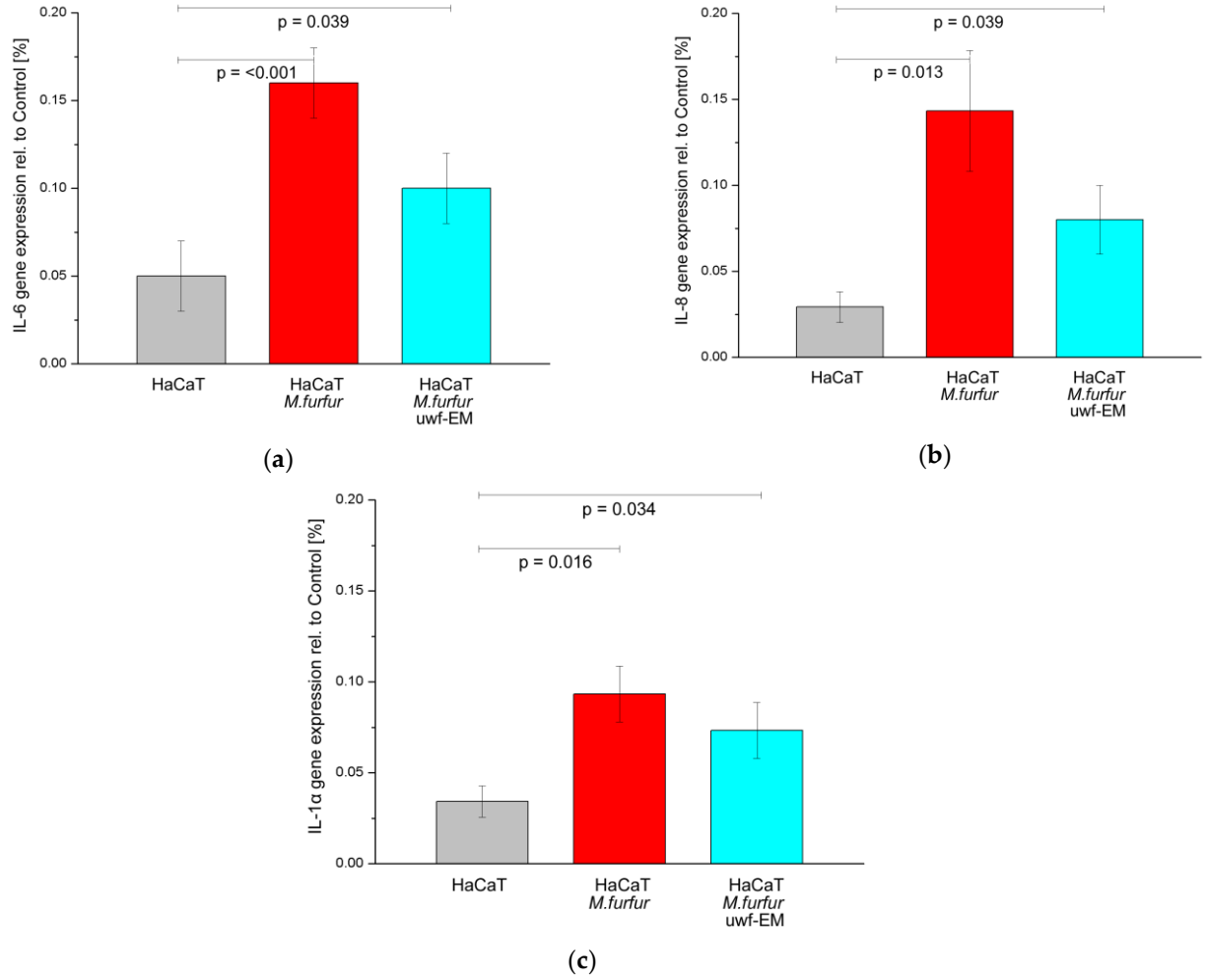

Figure 3. Gene expression of IL-6 (**a**), IL-8 (**b**), and IL-1α (**c**) of HaCaT cell cultures after 24 h of incubation. The figure depicts the control (grey), the batch infected with *M. furfur* (red), and the batch infected with pre-treated *M. furfur* that underwent uwf-EM exposure (blue). For further details, see the Methods section. The calculated *p*-values ($p < 0.05$) highlight the statistical significance of the obtained results.

Table 3. Numeric representation of pro-inflammatory cytokines compared to the control as averages of three replicates along with the corresponding standard deviations.

Gene	HaCaT	HaCaT + *M. furfur*	HaCaT + *M. furfur* + uwf-EM
IL-6	0.047 ± 0.014	0.160 ± 0.016	0.100 ± 0.016
IL-8	0.029 ± 0.007	0.143 ± 0.028	0.080 ± 0.016
IL-1α	0.034 ± 0.007	0.093 ± 0.012	0.073 ± 0.013

In contrast, in HaCaT infected batches with pre-treated *M. furfur* that underwent uwf-EM exposure, we observed that the IL-6 and IL-8 gene expressions fell again by 37.5% and 44.2%, respectively, when compared to HaCaT cultures infected with *M. furfur* not exposed to the uwf-EM field. IL-1α concentrations decreased to a lesser extent by 21.5%.

2.4. Effect of uwf-EM Signals on hBD-2

To investigate the expression of hBD-2, keratinocytes were infected for 24 h with and without uwf-EM pre-treated *M. furfur*. Following the 24 h incubation period, as shown in Figure 4 (respectively, Table 4), the batch infected with *M. furfur* that did not undergo

uwf-EM exposure resulted almost in double the hBD-2 compared to the HaCaT controls. The batch infected with *pre*-treated *M. furfur* that did undergo uwf-EM treatment almost tripled with respect to the HaCaT infected with *M. furfur* only.

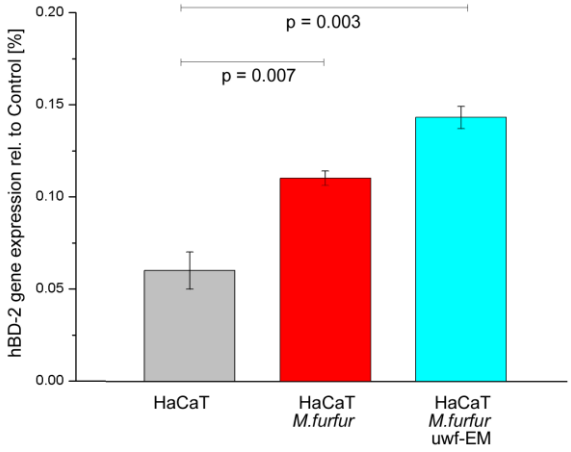

Figure 4. hBD-2 gene expression of HaCaT cell cultures after 24 h of incubation. The figure shows the control (grey), the batch infected with *M. furfur* (red), and the batch infected with pre-treated *M. furfur* that underwent uwf-EM exposure (blue). For further details, see the Methods section. The calculated *p*-values ($p < 0.05$) highlight the statistical significance of the obtained results.

Table 4. Numeric representation of the antimicrobial peptide compared to the control as averages of three replicates along with the corresponding standard deviations.

Gene	HaCaT	HaCaT + *M. furfur*	HaCaT + *M. furfur* + uwf-EM
hBD-2	0.060 ± 0.005	0.110 ± 0.004	0.143 ± 0.006

3. Discussion

Keratinocytes are the major constituent of the outermost epidermal layer and, as such, not only provide the keratin that gives human skin its strength, but also shield organisms from environmental pathogens. Under normal circumstances, the commensal fungus *Malassezia* spp. is part of a healthy cutaneous microbiome that colonizes the skin without causing harm. Yet in immunosuppressed individuals, the proliferation of this saprophyte can result in a wide range of skin-related disorders. Therefore, immortalised human keratinocytes (HaCaT) have been used to study the interaction of *M. furfur* in the presence of a low-intensity fractal electromagnetic signal in the ultra-low (ULF) to very-low frequency (VLF) bands. As both the fractal property and the low intensity of the applied field seem to contradict common sense and given the fact that the concept of hormesis still remains a challenge to the biomedical and clinical communities [29], a detailed look at these two aspects is given in the Appendix. Therein, we provide insight for a better understanding of the therapeutic implications of the hormetic dose–response relationships. In addition, we attempt to bridge the gap between hormesis and coherence in living matter, as was already addressed to some extent in our previous study [27].

Keratinocytes release cytokines after microbial stimulation, and *M. furfur* has repeatedly been shown to modulates the production of proinflammatory mediators in keratinocytes [30]. In the case of skin infection or injury, the expression of antimicrobial peptides is upregulated. Since the gene expression of hBD-2 is virtually absent in healthy skin, the expression in HaCaT cells can only be stimulated via the exposure of cutaneous pathogens or be induced by other environmental stressors [31].

In this study, we evaluated the ability of uwf-EM signals to modulate the hBD-2 gene expression in HaCaT cells. Our results showed that uwf-EM exposure of both *M. furfur* and infected HaCaT cells is able to increase the hBD-2 gene expression in keratinocytes by

a factor of ≈3 compared to the nonexposed controls. This is remarkable since defensins attract inflammatory cells, such as neutrophils, B-cells, and macrophages [32,33]. Furthermore, our experiments demonstrate that HaCaT cells respond with a strong increase in IL-6 and IL-8 gene expressions after 24 h following infection with *M. furfur* compared to untreated cells. In contrast, uwf-EM-treated *M. furfur* and infected HaCaT cells resulted in suppressed IL-6 and IL-8 gene expressions when compared to the *M. furfur*-infected HaCaT culture. In parallel, we examined the invasive capability of uwf-EM-treated *M. furfur* and demonstrated that the invasiveness of *M. furfur* was subsequently reduced by 35% compared to the non-uwf-EM-exposed controls. This finding suggests that treatment with uwf-EM signals has the potential to reduce the incidence of systemic mycosis.

Our results also suggest that the huge upregulation of hBD-2 following exposure to the uwf-EM field represents one of the primary innate immune responses against microorganisms such as *M. furfur*. As expected, proinflammatory cytokines, such as IL-6, IL-8, and IL-1α, as well as the antimicrobial peptide hBD-2 are upregulated upon infection with *M. furfur*. Exposure with uwf-EM treatment, however, supresses the gene expression of cytokines, while the expression of the antimicrobial peptide is further stimulated.

In terms of the potential medical applications, keratinocytes are an ideal model for analysing the biological effects of ultra-weak (low-intensity) nonionizing ULFs/VLFs. Elucidating a deeper understanding of the mechanisms could lead to novel nonchemically based methods against *M. furfur* infection. From a therapeutic perspective, uwf-EM exposure could be used as a basic treatment in conjunction with conventional therapy when treating *M. furfur*. As interesting as these results may be, further in vivo studies are necessary to understand the physicochemical processes triggered by these fields. Promising examples utilizing similar approaches are currently in the making and concern the use of pulsed magnetic field treatment for diabetic cells [34] and narrow-band electromagnetic field exposure in containing COVID-19 [35] as well as altering the proton density and ATP synthase rotation in the context of mitochondrial dysfunction, as often observed in tumour biology [36]. In fact, tumour-treating fields are already used in some medical fields. These rely on the application of a 1–3 V/cm (0.335–1.005 μT) field in the β-dispersion regime (100–300 kHz) to induce a regression in glioblastomas by adversely affecting the microtubule assembly during mitotic events [37].

4. Materials and Methods

4.1. Microorganisms and Culture Media

Malassezia furfur ATCC 12078 was obtained from the American Type Culture Collection (Rockville, MD, USA). *M. furfur* was grown for 4 days at 30 °C in Sabouraud's dextrose agar containing peptone (1%), glucose (4%), olive oil (2.0%), and Tween 80 (0.2%).

4.2. Cell Culture and Treatments

Aneuploid immortal keratinocytes (HaCaT) from adult human skin were plated in 6-multiwell plates (35 mm diameter) with 2 mL of Dulbecco's modified Eagle medium (DMEM) supplemented with 10% foetal bovine serum, 100 U/mL penicillin, 100 μg/mL streptomycin, and 2 mM L-glutamine at 37 °C and 5% CO_2.

M. furfur was washed three times in phosphate-buffered saline (PBS). The resulting precipitate was resuspended in a small volume of Dulbecco's modified Eagle medium (DMEM) and vortexed gently to avoid yeast aggregation. Thereafter, one batch of *M. furfur* designated for the exposure trials was treated for 10 min under dark conditions with the uwf-EM-generating device at a working distance of 8 cm from the culture. The control batch was handled in the same way but was sham-exposed (i.e., the uwf-EM device was disabled). The exposure procedure was conducted on a tray-like setup where the antenna was placed atop, while the biological samples were placed below using a working

distance of 80 mm. Since proper field propagation is essential, it was of paramount importance that no ferromagnetic material was located nearby. To ensure a standardized uwf-EM field exposure, a fully digitized prototype was used. This field-generating device was based on the WHITE holographic bioresonance method [24] and consists of a logarithmic coil printed on a circuit board. This "antenna" is supplied with a VLF/ULF audio signal which has fractal characteristics. Only a fully digitized approach allows for standardized field exposures. In order to achieve this, a computer-based solution (Rasbperry-Pi®) was chosen, which allows the user to select the proper fractal audio file via menu-guided options. Thus, the signal-generating source consists of three sub-units: (i) the processor board, (ii) the touchscreen, and (iii) the high-end D/A converter. Together with the PCB antenna, it forms a unit we refer to as FRACTOS (for more details see [27]). Incubation following uwf-EM treatment was executed in separate compartments of the incubator to avoid electromagnetic crosstalk, which could induce artifacts [38].

Yeast viability was assessed using standard colony-forming unit (CFU) counts. Human keratinocytes were treated with *M. furfur* at a ratio of 30:1, were likewise treated with the uwf-EMF signal using the same device (except the controls), and were incubated for up to 96 h. A simplified process flow diagram (not showing the uwf-EM treatment of the *M. furfur* culture) can be seen in Figure 5. Since cell proliferation rate of the keratinocytes was similar to that of the uninfected controls, it can be assumed that the vitality of the keratinocytes is not affected by *M. furfur*. After 24 h and 48 h, the keratinocytes were processed for RNA extraction. Morphological features of HaCaT cells were defined by phase-contrast microscopy using an Olympus CDK40 at 20× magnification (not shown).

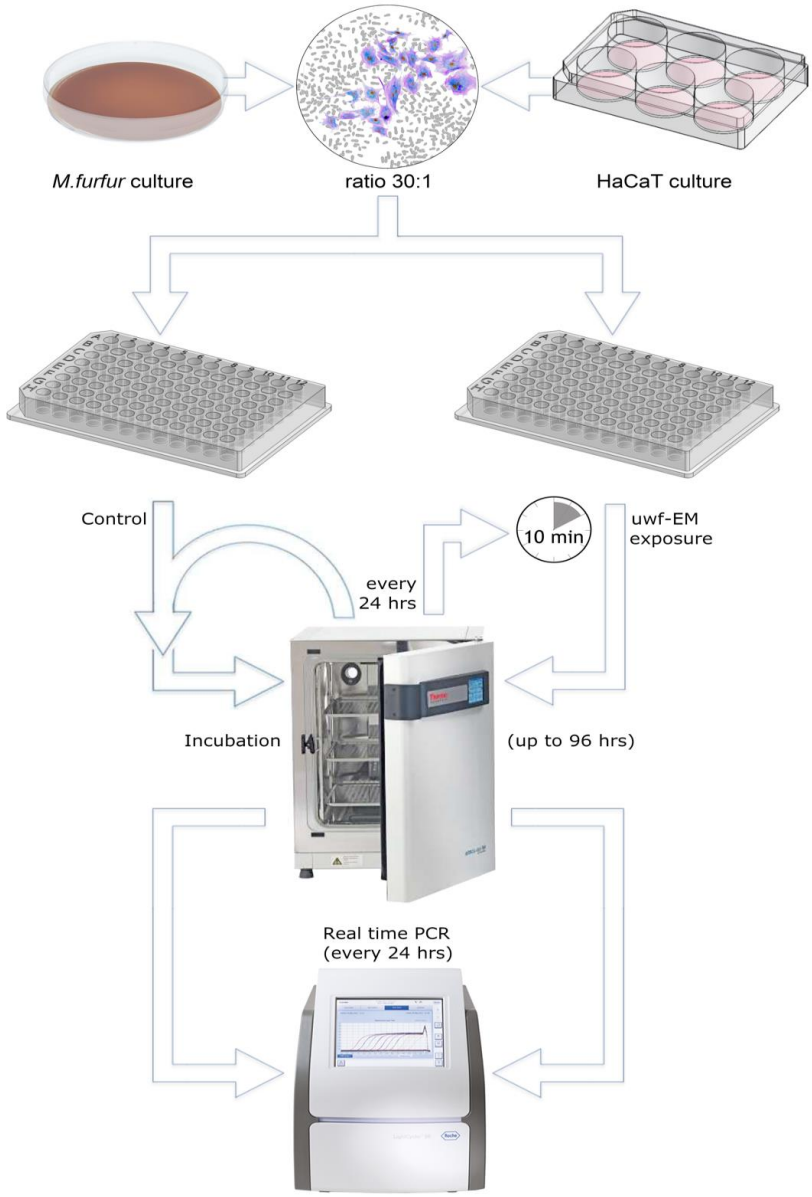

Figure 5. Simplified sketch of the performed protocol. HaCaT cells were cultivated in 6-well plates, whereas *M. furfur* was cultivated on Sabouraud agar in a 100 mm Petri dish. Initially, fungal cultures were uwf-EM pre-treated for 10 min (at a distance of approx. 80 mm from the log antenna), while controls were not treated (not shown in the figure). Infection of keratinocytes with the yeast was performed in 6-well plates (35 mm) at a ratio of about 30:1. Thereafter, incubation of infected and uninfected cell cultures for up to 96 h started. HaCaT viability was assessed by an MTT assay, while the gene expressions of IL-6, IL-8, and IL-1α were performed using RT-PCR. Every 24 h, the charge to be tested was uwf-EM-exposed for 10 min followed by another cycle of incubation with the same distance parameters mentioned above.

4.3. MTT Cell Proliferation Assay

The metabolic activity was measured using an MTT assay. HaCaT cells were grown in microplates (tissue culture grade, 96 wells, flat bottom) in a final volume of 100 µL of DMEM at 37 °C and 5% CO_2. After 24 h of treatment, 10 µL of 3-(4,5-dimethylthiazol-2-yl)-2,5-diphenyltetrazoliumbromide (MTT) labelling reagent (Roche Diagnostics, Basel, Switzerland; final concentration 0.5 mg/mL) was added to each well. Following the procedure according to [39], 100 µL of the solubilization solution (10% SDS in 0.01 M HCl) was added to the culture after 4 h and was incubated overnight. The spectrophotometric absorbance was measured using a microplate ELISA reader (Biorad) at a 570 nm

wavelength as the conversion from yellow tetrazole to purple formazan by the living cells is best seen at this bandwidth.

4.4. Microorganisms and Culture Media

To distinguish between uwf-EM-treated and untreated *M. furfur*, two parallel batches of semi-confluent keratinocytes (106/well) were needed and infected with *M. furfur*. After 24 h of incubation, the total RNA content was isolated using the High Pure RNA Isolation Kit (Roche; Milan, Italy). Approximately 200 ng of the total cellular RNA was reverse transcribed (Expand Reverse Transcriptase, Roche; Milan, Italy). Transcription into complementary DNA (cDNA) using random hexamer primers (Random hexamers, likewise from Roche) occurred at 42 °C for 45 min. Real-time PCR was carried out with the LC Fast Start DNA Master SYBR Green kit (Light Cycler 2.0 Instrument, also from Roche) using 2 mL of cDNA, corresponding to 10 ng of total RNA, in a final volume of 20 mL to which 3 mM $MgCl_2$ and 0.5 mM sense and antisense primers were added (Table 5). A melting curve was produced at the end of each amplification to ensure that no nonspecific reaction products were present. As the accuracy of mRNA quantification depends on the linearity and efficiency of the PCR amplification, both parameters were assessed using standard curves generated by increasing amounts of cDNA. Quantification was based on the threshold cycle values measured at the early stage of the exponential phase of the reaction. Normalization to the internal standard curve with the β-actin gene was also performed to avoid discrepancies in the input RNA or reverse transcription efficiency. Finally, PCR products were examined in a 1.4% agarose gel electrophoresis.

Table 5. Sense and antisense primers of the five gene sequences showing sense (upper row) and antisense strands (lower row).

Gene	Primer Sequence	Conditions	Product Size (bp)
IL-6	5′-CTC CAG CAT CCG ACA AGA AGC-3′ 5′-GAG GTC GTA GGC TGT TCT TCG-3′	1′ at 94 °C, 1′ at 63 °C, 1′ at 72 °C for 33 cycles	234
IL-8	5′-ATG ACT TTC AAG CTG GCC GTG-3′ 5′-TGA ATT CTC AGC CCT CTT CAA AAA CTT CTC-3′	1′ at 94 °C, 1′ at 56 °C, 1′ at 72 °C for 33 cycles	297
hBD-2	5′-CCA GCC ATC AGC CAT GAG GGT -3′ 5′-AAC CGG TAG TCG GTA CTC CCA-3′	1′ at 94 °C, 1′ at 63 °C, 1′ at 72 °C for 33 cycles	254
IL-1α	5′-CCG ACT ACT ACG CCA AGG AGG TCA CGT-3′ 5′-AGG CCG GTT CAT GCC ATG AAT GGT GCA-3′	1′ at 94 °C, 1′ at 60 °C, 2′ at 72 °C for 32 cycles	439
β-actin	5′-TGA CGG GGT CAC CCA CAC TGT GCC CAT CTA-3′ 5′-CTA GAA GCA TTG CGG GTG GAC GAT GGA GGG-3′	30″ at 95 °C, 1″ at 56 °C, 30″ at 72 °C for 35 cycles	661

4.5. Invasion Assay for Malassezia furfur

Human keratinocytes were infected with and without uwf-EM-treated *M. furfur*. Infection occurred at a dilution rate of 30:1 (yeast-to-keratinocyte ratio, as proposed by Donnarumma et al. [40]) for 24 and 48 h. To remove nonadherent yeast cells, the keratinocytes were washed three times with PBS. The infected keratinocytes were successively treated with 1 mL of DMEM containing ketoconazole at the micocidal concentration and were incubated for 4 h at 37 °C. The infected cells were then treated with trypsin-EDTA for 5 min at 37 °C and lysed by adding 1 mL of cold 0.1% Triton-X100. The cell lysates were diluted in PBS, plated on Sabouraud–dextrose agar, and incubated for 72 h at 30 °C. The viable intracellular yeast content was then determined and plotted as a concentration ml^{-1}.

4.6. Statistical Analysis

Both experiments and measurements were performed in triplicate, enabling basic statistics. Beginning with the magnetic flux density measurements, the results are expressed in Table 6 as mean ± standard deviations (±SD). The measurements were taken using an NFA-1000 magnetometer with an integrated data logger (GHz-Solutions, FRG) and were processed with the software packages (NFAsoft v.1.72 from the same supplier). Due to the weak signals irradiated from the antenna, the measurements were performed inside a mu-metal test chamber (Marchandise-Tech, FRG) specifically designed for this type of investigation. For all exposure trials, the following uncompressed source file was used: S1_20-24_bit 48k_with_cutoff_500 Hz.wav.

Table 6. Magnetic flux densities of the background with the antenna in operation stated as averages along with standard deviations of three replicates. Background values denote the signal strength with both the inactivated antenna and cell culture placed in the mu-metal test box, whereas uwf-EM measurements denote the emitted field intensities when the antenna was operational.

Trials	Min	Max	Avg	Stdev	95th%ile	Unit
Backgnd.	0.500 ± 0.001	3.033 ± 0.808	0.967 ± 0.023	0.377 ± 0.040	1.680 ± 0.125	[nT]
uwf-EM	7.133 ± 0.379	12.567 ± 0.208	9.310 ± 0.141	0.580 ± 0.040	10.260 ± 0.185	[nT]

To estimate the effect size of the CFUs of *M. furfur*, Cohen's "d" was determined. According to Cohen's conventions, there is a significant difference in the means if d > 1. For both the uwf-EM-exposed and *M. furfur* in contact with HaCaT cells, values of 3.56 (uwf-EM "on/off") and 2.46 (uwf-EM "on/off" when in contact with HaCaT cells) standard deviations were obtained.

Assuming that the repetitive trials belong to a Gaussian distribution, the probability was determined using a *t*-test and the corresponding *p*-value. For this purpose, a standard significance level alpha (α) of 0.05 was defined. For all the graphs in the figures above, it can be shown that the probability that a random gene expression could have provoked the differences is extremely low and that the results obtained are indeed significant differences with regard to the controls.

To determine the statistical significance of the PCR gene expression results an ANOVA test (analysis of variance between groups) was used (Table 7). The hypothesized mean difference (with H_0 stating that there is no difference between means) was set to zero. As with the above case, a standard alpha level (α) 0.05, or 5%, was chosen. The *p*-value for the proinflammatory response of the yeast-infected HaCaT cells was found to be <0.002, confirming the statistical significance of the results. It was also found that the antimicrobial and cytotoxic peptide in the form of hBD-2 fluctuated to some extent in the controls, whereas the yeast-infected and uwf-EM-treated keratinocytes showed a somewhat stabilized defensin production. The documented differences are significant, suggesting that yeast infection and uwf-EM treatment do indeed upregulate the hBD-2 expression.

Table 7. Single-factor ANOVA test. With reference to the figures above, the divergent trends of the HaCaT controls, the cultures infected with *M. furfur*, and the cultures also exposed to uwf-EMF yield significant differences at a significance level of $p < \alpha$ (0.05). Accordingly, H_0 was rejected for IL-6, IL-1α, IL-8, and hBD-2, as confirmed by the corresponding F-values, which are much greater than those of F_{crit} (>5.143).

ANOVA	F	*p*	F_{crit}
IL-6	22.750	0.002	5.143
IL1-α	14.978	0.005	5.143
IL-8	17.124	0.003	5.143
hBD-2	119.647	<0.001	5.143

5. Conclusions

Malassezia furfur is a yeast fungus that is an integral part of an intact skin microbiome (present in more than 90% of adult humans). However, in stressed individuals and due to environmental factors, it can occur as an opportunistic pathogen. Therefore, its presence is considered important in the etiology of skin disorders such as *Pityriasis versicolor* and *Seborrheic dermatitis*. *M. furfur* was collected from adult individuals by swabbing and was transferred to Sabouraud agar, placed in saline solution, and exposed for 10 min to an uwf-EM field.

The pre-treated yeast (for the exposure trials) and the untreated yeast (for the controls) were used to infect HaCaT cells (immortalised human keratinocytes) at a ratio of 30:1. The infected cells were incubated for up to 96 h, were repeatedly uwf-EM-exposed, and were repeatedly processed for RNA extraction to assess their gene expression for markers normally involved in the inflammatory process as a result of *M. furfur* infection. In this study, the application of uwf-EM stimuli was shown to have regulatory effects on gene expression, which was reflected in the reduced invasiveness of *M. furfur* without drastically affecting the growth dynamics in HaCaT cells. Considering the very low intensities of the applied uwf-EM signals, we can clearly label the EM-induced effect as hormetic. The low-intensity stimulation induced cellular adaptations, as previously observed by Vaiserman [41], and stimulated protein activation in the living system, documented by Kim et al. [42]. Although the uwf-EM exposure time between incubation cycles was quite short (10 min each), it was apparently sufficient to induce a genetic adaptation response. This led to a long-lasting memory effect (probably of epigenetic origin) that needs to be investigated in future studies. In turn, it renders adaptive responses more efficiently and corroborates a positive hormetic feedback principle. The use of uwf-EM agents (hormetins) offers a fascinating area for further research, with reprogramming of the epigenome to reestablish a homeostatic healthy steady state. This has the potential to become the method of choice as the undesired side effects so often observed with biochemical agents can be minimized.

Supplementary Materials: The following supporting information can be downloaded at: https://www.mdpi.com/article/10.3390/ijms24044099/s1.

Author Contributions: Conceptualization, A.T. and P.M.; investigation, A.T. and P.M.; methodology, R.G. and A.T.; writing—original draft preparation, P.M.; writing—review and editing, H.L.; data curation, R.G.; project administration, H.L. All authors have read and agreed to the published version of the manuscript.

Funding: This work was supported by grants from a liberal donation by Pietro Elli.

Institutional Review Board Statement: Not applicable as this study did not involve experimental trials with humans or animals.

Informed Consent Statement: Not applicable.

Data Availability Statement: The data presented in this study are available in Supplementary Material.

Acknowledgments: Special thanks to Anna De Filippis (Department of Experimental Medicine, Section of Microbiology and Clinical Microbiology, University of Campania "L. Vanvitelli" Naples, Italy) who carefully monitored and intervened during the experimental work whenever it was necessary. We want to express our thanks to Maria Antonietta Tufano (from same Department) for enabling us to perform these biophysical trials in her laboratories. We appreciate the support received by Andreas Feichtner (Department of Physics and Biophysics, University of Salzburg, Austria) for programming the FRACTOS device as well as the 3D-printing support for the FRACTOS housing performed by Andreas Schroecker (Design & Product Management, University of Applied Science, Puch, Austria). Additional thanks are expressed to Giuseppe Vitiello (Dep. of Physics, University of Salerno, Italy) for useful discussions during the compilation of the manuscript. Finally, we dedicate this writing to our beloved friend and courageous pioneer Emilio Del Giudice who has been a passionate supporter of the unity of Nature, Science, and Art.

Conflicts of Interest: The authors declare no conflict of interest.

Appendix A. Hormesis in Low-Intensity EM Fields and Its Relation to QED

In the past, HaCaT were exposed to a continuous 50 Hz sinusoidal magnetic field for up to 96 h at a flux density of 2 mT, resulting in an increase in cell proliferation (in vitro, cells reached confluence sooner compared to unexposed controls) and a greater clonogenic capacity [43]. In contrast, human oral keratinocytes exposed to the same field for the same duration resulted in a decrease in cell proliferation and a reduction in clonogenic capacity [44]. While the latter seems to be more in line with the hormetic principle, the former tends to contradict it. However, a closer look at these contrasting results reveals that irradiation causes a rearrangement of actin filaments, leading to an increase in actin expression and in the formation of stress fibres crossing parallel to the elongated cells along with a decreased expression of the EGF receptor [44].

Although a direct comparison with the current study is not really possible—as here HaCaT cells were not only inoculated with a yeast strain, but also, the applied field-intensities were almost three orders of magnitude lower—visible effects are nevertheless evident. One could argue that the results presented here comply with the linear no-threshold (LNT) hypothesis as postulated for the effects of ionizing radiation—indeed, the ICRP continues to recommend the use of the LNT hypothesis for the development of prospective radiation control programs [45]. Yet, it is widely recognized that the LNT hypothesis is incompatible with an organism's positive response to a toxic agent because it would imply the existence of a threshold in the concentration–effect curve. Another incompatibility with the LNT hypothesis concerns the impossibility of an adaptive biological response to counteract or neutralise the effect of radiation [46].

Does the mechanism underlying the observed effects of such "weak" stimuli justify to speak of hormesis? The phenomenon itself has been known since the late 19th century in the form of the Arndt–Schulz Law (ASL). It states that, "every substance which can paralyze or kill any cell or cell protoplasm can also act in small quantities …. as a stimulus to cell activity" [47], or simply "the potency of remedies might increase with their dilution" [46]. Nowadays this law is synonymous with hormesis and is defined as a biphasic dose–response phenomenon (as shown in Figure A1). It is characterized by a low-dose stimulation and a high-dose inhibition [48]. Hormesis, so far, has been extensively investigated in the context of chemical toxins [49] but hardly when dealing with physical eu/distressing agents—except for ionizing radiation [50].

Psychophysics deals with human perception (vision, hearing, taste, touch, and smell), the relation between the actual change in a physical stimulus, and the perceived change [51]. Here, "the minimum increase of stimulus which will produce a perceptible increase of sensation is proportional to the pre-existent stimulus" [52]. This principle, first established by Weber and later mathematically derived by Fechner, became widely known in sensory physiology as the Weber–Fechner law (WFL).

With reference to these two laws and the fact that electromagnetic radiation involves the application of an energy field or phase correlation, one could be inclined to argue that the WFL is more comprehensive and, as such, is more compatible with the study results herein presented. Indeed, such a peculiar dose–response pattern was demonstrated already about 50 years ago using mm-wave frequencies [53] where low-power flux densities (few mW/cm^2) significantly altered the cell divisions of microorganisms. The authors back then concluded that the biological response is frequency rather than power dependent.

In a recently published study [34], the authors reported statistically significant cellular responses with pulsed magnetic field stimuli in the range from 1–250 μT with frequencies in the range from 1–250 Hz. Such pulses can be used to induce tissue regeneration on chronic and difficult-healing wounds. Although the field intensities in that study were three orders of magnitude higher than those presented in this study, the obvious nonthermal efficacy of the pulsed ELF/SLF is remarkable.

In fact, ULF/VLF fields with higher intensities (>1 μT) are known to induce distressing effects such as free radical build-up, while even higher field intensities (>1 mT) stimulate cell proliferation, altered viability, and differentiation as well as DNA-strand brakes [54–56]. Exposure to low-intensity fields on the other hand, stimulates eustress responses [19,57–59]. Regardless of the underlying principle (ASL vs. WFL), we are dealing here with a hormetic effect as the dose–response patterns is indeed biphasic, as can be seen in Figure A1. Therein, the authors [60] investigated the minimal field strength required to induce hyperfine and degenerative effects, i.e., the experiment consists of perturbing the spin dynamics arising from the Zeeman interaction of the radicals with an external magnetic field that can either accelerate or slow down the intersystem transition between singlet and triplet states. Although the authors do not explicitly refer to the peculiar behaviour at low magnetic field intensities (<2 mT), the dynamics obtained suggest hormetic principles in action. The superimposition of the static field (B_{DC}) with a weak ELF (B_{AC} with certain frequencies) acts constructively via harmonic coupling such that the induced effects acting on the cyclotron resonance of specific ions can be derived with B_{AC} fields down to the nT range [61]. In addition, hormetic dynamics can be used as a predictor to indicate the lowest values of a substance or agent (e.g., applied magnetic field) that exhibit inhibitory or stimulating effects [62].

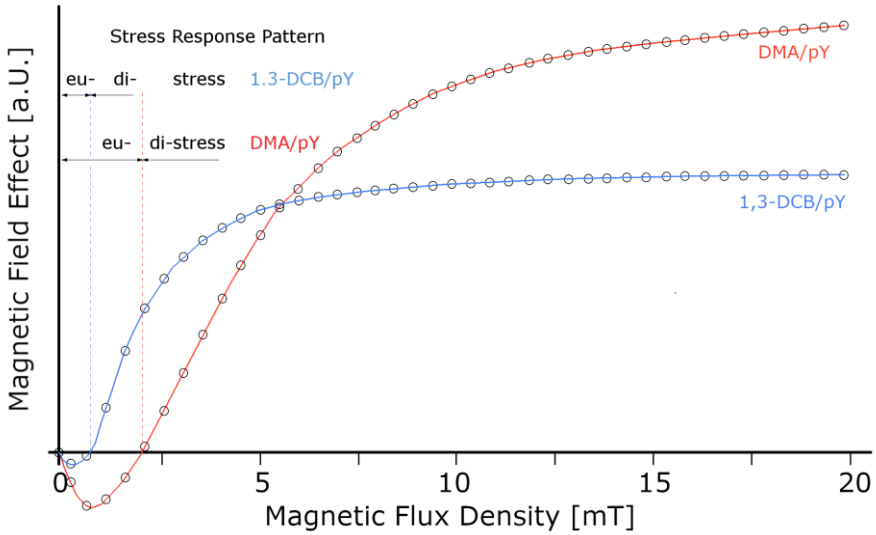

Figure A1. Curves of the modelled magnetic field effects of exciplex systems consisting of pyrene and isomers of dicyanobenzene (1,3- dicyano-benzene (DCB) or dimethyl-aniline (DMA)) (redrawn and modified after [60]). Superimposed, the eustress and the corresponding distress response regimes indicating that weak field stimuli promote, whereas strong field stimuli inhibit.

A similar effect could be documented using single-celled algae in cultures [63]; therein, the authors consistently observed that higher alternating magnetic field intensities (200 μT) suppressed algal growth, while lower ones (20 μT) stimulated algal proliferation. The effects of ELF fields seem to be frequency dependent and are determined by so-called resonance frequencies [64]. Similarly, it was possible to stimulate ultra-weak photon emissions in the visible range in *Arabidopsis thaliana* by a combination of a static magnetic field (55–65 μT) coupled to an alternating magnetic field [65]. Again, the hormetic principle was observed as higher B_{AC} intensities resulted in the suppression of bio-photonic emissions. Regarding the cyclotron resonance of Ca^{2+} ions, which is crucial for all life processes, it was demonstrated in an aqueous solution containing the membrane lipid L-α-phosphatidylcholine that the optimal strength of B_{AC} was 150 nT as long as the static magnetic field B_{DC} was set to 65 μT [66]. Again, the hormetic principle was evident as intensities below and above 150 nT resulted in weaker rotation rates of the ion.

The biphasic behaviour becomes particularly clear when viewed from the perspective of quantum electrodynamics (QED) where the observed behaviour becomes a logical consequence. Essentially, QED deals with how light (electromagnetic field) and matter (charged particles) interact via the exchange of virtual photons. The description of condensed matter using a nonperturbative QED approach, focussing in particular on liquid water, was undertaken by Preparata [67] who laid the foundations for an elegant reinterpretation of the concept of "hydrogen bonding". Water, viewed from the QED perspective, predicts the oscillatory modes between the ground state and the excited state of the oxygen atom (5d-level) located 12.07 eV [68]. Since this oscillation is energetically more favourable than the decoherent ground state, a large amount of water molecules collectively flip into this state. The resulting collective in-phase oscillation within clusters leads to coherent domains (CDs) that remain unaffected by thermal assault, even when water changes into the gaseous phase [69]. In the context of QED, resistance to thermal assault—known as the "K_BT problem" [70]—is fundamental as it highlights the incredibly low energy requirements of living systems [71]. Indeed, there is ample experimental evidence for sub-k_BT effects; in particular, weak coherent EMF signals have been found to be effective in spite of the ubiquitous endogenous noise—see the review of [72]. Therein, the author lists a wide range of interaction mechanisms, such as ion cyclotron, ion paramagnetic, and ligand–receptor binding resonances, that use energy levels well below k_BT.

As predicted by Preparata [67] and later corroborated by Garbelli [69], coherence in aqueous systems exhibits a biphasic property of water, so much so that the liquid phase exists in two fractions: a coherent fraction (F_C), consisting of an ensemble of CDs, and a non-coherent fraction (F_{nC}), prevailing at the boundary layer and between CDs [73]. Not surprisingly, these two coexisting fractions of water have different densities [74]. Apparently, the ratio between F_C and F_{nC} ($F_c(T) = 1 - F_n(T)$) is temperature dependent and has been calculated to be 80% coherent at 200 K (solid phase), 40% at 300 K (liquid phase), and about 10% coherent at 550 K (gaseous phase) [69]. Consequently, water CDs, whose size is the wavelength of 100 nm (correspond to an energy level of 12.07 eV), become a reservoir of both quasi-free electrons at the CDs' periphery and a corresponding fraction of quasi-free protons within the CDs. This charge separation is of crucial importance as we follow Marchettini's interpretation that once a CD is immersed in an energy field, it becomes recharged, maintaining a permanent oscillation in which charging is electromagnetic (essentially via hormetic intensities) and discharging is chemical (triggering biochemical reactions) [75]. The relevance of these far-reaching properties for our investigation becomes clearer when the electromagnetic nature of the biological dynamics and the central role of water are confronted with experiments showing that serial dilutions generate ULF fields (500–3000 Hz) when exposed to ELF noise (Schumann frequencies), as regularly found in nature [76]. Therefore, additional evidence corroborating these phenomena is given also by a number of other experiments performed in the past [77]. For a better understanding of the specificity of this phenomenon and its relation to hormesis, we ask the reader to be patient as we are in the process of compiling a paper that highlights exactly this particular issue.

References

1. Schoch, C.L.; Ciufo, S.; Domrachev, M.; Hotton, C.L.; Kannan, S.; Khovanskaya, R.; Leipe, D.; Mcveigh, R.; O'Neill, K.; Robbertse, B.; et al. NCBI Taxonomy: A comprehensive update on curation, resources and tools. *Database* **2020**, baaa062. https://doi.org/10.1093/database/baaa062. Available online: https://www.ncbi.nlm.nih.gov/Taxonomy/Browser/wwwtax.cgi?id=55194 (accessed on 23 April 2021).
2. Harada, K.; Saito, M.; Sugita, T.; Tsuboi, R. Malassezia species and their associated skin diseases. *J. Dermatol.* **2015**, *42*, 250–257. https://doi.org/10.1111/1346-8138.12700.
3. Ashbee, H.R. Update on the genus Malassezia. *Med. Mycol.* **2007**, *45*, 287–303. https://doi.org/10.1080/13693780701191373.
4. Difonzo, E.M.; Faggi, E.; Bassi, A.; Campisi, E.; Arunachalam, M.; Pini, G.; Scarfì, F.; Galeone, M. Malassezia skin diseases in humans. *Giorn. Ital. Dermatol. Venereol*. **2013**, *148*, 609–619.

5. Clausen, M.L.; Agner, T. Antimicrobial Peptides, Infections and the Skin Barrier. *Curr. Probl. Dermatol.* **2016**, *49*, 38–46. https://doi.org/10.1159/000441543.
6. Kesavan, S.; Walters, C.E.; Holland, K.T.; Ingham, E. The effects of Malassezia on pro-inflammatory cytokine production by human peripheral blood mononuclear cells in vitro. *Med. Mycol.*, **1998**, *36*, 97–106. https://doi.org/10.1080/02681219880000161.
7. Niyonsaba, F.; Ushio, H.; Nakano, N.; Ng, W.; Sayama, K.; Hashimoto, K.; Nagaoka, I.; Okumura, K.; Ogawa, H. Antimicrobial peptides human-defensins stimulate epidermal keratinocyte migration, proliferation and production of proinflammatory cytokines and chemokines. *J. Invest. Dermatol.* **2007**, *127*, 594–604. https://doi.org/10.1038/sj.jid.5700599.
8. Ishibashi, Y.; Sugita, T.; Nishikawa, A. Cytokine secretion profile of human keratinocytes exposed to Malassezia yeasts. *FEMS Immunol. Med. Microbiol.* **2006**, *48*, 400–409. https://doi.org/10.1111/j.1574-695X.2006.00163.x.
9. Baroni, A.; Orlando, M.; Donnarumma, G.; Farro, P.; Iovene, M.R.; Tufano, M.A.; Buommino, E. Toll-like receptor 2 (TLR2) mediates intracellular signalling in human keratinocytes in response to Malassezia furfur. *Arch. Dermatol. Res.* **2006**, *297*, 280–288. https://doi.org/10.1007/s00403-005-0594-4.
10. Hazlett, L.; Wu, M. Defensins in innate immunity. *Cell. Tissue Res.* **2010**, *343*, 175–188. https://doi.org/10.1007/s00441-010-1022-4.
11. Wainwright, M.; Maisch, T.; Nonell, S.; Plaetzer, K.; Almeida, A.; Tegos, G.P.; Hamblin, M.R. Photoantimicrobials—Are we afraid of the light? *Lancet Infect. Dis.* **2017**, *17*, e49–e55. https://doi.org/10.1016/S1473-3099(16)30268-7.
12. Mattson, M.P. Hormesis defined. *Ageing Res Rev.* **2008**, *7*, 1–7. https://doi.org/10.1016/j.arr.2007.08.007.
13. Ayrapetyan, S.N.; Markov, M.S. Bioelectromagnetics Current Concepts. In *NATO Security through Science Series*; Series B.; Springer: Dodrecht, The Netherlands, 2006. https://doi.org/10.1007/1-4020-4278-7.
14. Becker, R.O.; Marino, A.A. *Electromagnetism and Life*; New York State University Press: Albany, NY, USA, 1982. ISBN: 978-0981-8549-08.
15. Koenig, H.L.; Krueger, A.P.; Lang, S.; Sonning, W. *Biologic Effects of Environmental Electromagnetism*; Springer: Berlin, Germany, 1981. https://doi.org/10.1007/978-1-4612-5859-9.
16. Marha, K.; Musil, J.; Tuha, H. *Electromagnetic Fields and the Life Environment*; San Francisco Press: San Francisco, CA, USA, 1971. ISBN: 91-1302-13-7.
17. Marino, A.A. *Modern Bioelectricity*; CRC Press: Boca Raton, FL, USA, 1988. https://doi.org/10.1201/9781003065821.
18. Markov, M.S. *Electromagnetic Fields in Biology and Medicine*; CRC Press: Boca Raton, FL, USA, 2015. https://doi.org/10.1201/b18148.
19. Presman, A.S. *Electromagnetic Fields and Life*; Springer: New York, NY, USA, 1970. https://doi.org/10.1007/978-1-4757-0635-2.
20. Smith, C.W.; Best, S. *Electromagnetic Man—Health and Hazard in the Electrical Environment*; St. Martin's Press: New York, NY, USA, 1989. ISBN: 978-0312-0373-07.
21. Zhadin, M.N. Review of russian literature on biological action of DC and low-frequency AC magnetic fields. *Bioelectromagnetics*. **2001**, *22*, 27–45. https://doi.org/10.1002/1521-186x(200101)22:1<27::aid-bem4>3.0.co;2-2.
22. Binhi, V.N. Принципы электромагнитной биофизики (Principles of Electromagnetic Biophysics–in Russian); FIZMATLIT: Moscow, Russian, 2011; ISBN 978-5-9221-1333-5.
23. Schroedinger, E. *What Is Life? The Physical—Aspect of the Living Cell*, 13th ed.; Cambridge University Press: Cambridge, UK, 1944. ISBN: 978-1-107-60466-7.
24. Tedeschi, A. Is the Living Dynamics able to Change the Properties of Water? *Int. J. Design. Nat. Ecodyn.* **2010**, *5*, 60–67. https://doi.org/10.2495/DNE-V5-N1-60-67.
25. Del Giudice, E.; De Filippis, A.; Del Giudice, N.; Del Giudice, M.; d'Elia, I.; Iride, L.; Menghi. E.; Tedeschi, A.; Cozza, V.; Baroni, A.; Tufano, M.A. Evaluation of a Method Based on Coherence in Aqueous Systems and Resonance-Based Isotherapeutic Remedy in the Treatment of Chronic Psoriasis Vulgaris. *Curr. Top. Med. Chem.*, **2015**, *15*, 542–548. https://doi.org/10.2174/1568026615666150225103903.
26. Voeikov, V.; Del Giudice, E. Water respiration: The base of the living state. *Water* **2009**, *1*, 52–75. https://doi.org/10.14294/WATER.2009.4.
27. Madl, P.; De Filippis, A.; Tedeschi, A. Effects of ultra-weak fractal electromagnetic signals on the aqueous phase in living systems: A test-case analysis of molecular rejuvenation markers in fibroblasts. *Electromagn. Biol. Med.* **2020**, *39*, 227–238. https://doi.org/10.1080/15368378.2020.1762634.
28. Vitiello, G. Fractals, coherent states and self-similarity induced noncommutative geometry. *Phys. Lett. A* **2012**, *376*, 2527–2532. https://doi.org/10.1016/j.physleta.2012.06.035.
29. Calabrese, E.J. Resveratrol commonly displays hormesis: Occurrence and biomedical significance. *Hum. Experim. Tox.* **2010**, *29*, 980–1015. https://doi.org/10.1177/0960327110383625.
30. Schiller, M.; Metze, D.; Luger, T.A.; Grabbe, S.; Gunzer, M. Immune response modifiers—Mode of action. *Exp. Dermatol.* **2006**, *15*, 331–341. https://doi.org/10.1111/j.0906-6705.2006.00414.x.
31. Liu, L.; Roberts, A.A.; Ganz, T. By IL-1 signaling, monocyte-derived cells dramatically enhance the epidermal antimicrobial response to lipopolysaccharide. *J. Immunol.* **2003**, *170*, 575–580. https://doi.org/10.4049/jimmunol.170.1.575.
32. Baroni, A.; Perfetto, B.; Paoletti, I.; Ruocco, E.; Canozo, N.; Orlando, M.; Buommino, E. Malassezia furfur invasiveness in a keratinocyte cell line (HaCaT): Effects on cytoskeleton and on adhesion molecule and cytokine expression. *Arch. Dermatol. Res.* **2001**, *293*, 414–419. https://doi.org/10.1007/s004030100248.

33. Elsbach, P. What is the real role of antimicrobial polypeptides that can mediate several other inflammatory responses? *J. Clin. Investig.* **2003**, *111*, 1643–1645. https://doi.org/10.1172/JCI18761.
34. Zanotti, F.; Trentini, M.; Zanolla, I.; Tiengo, E.; Mantarro, C.; Dalla Paola, L.; Tremoli, E.; Sambataro, M.; Sambado, L.; Picari, M.; et al. Playing with Biophysics: How a Symphony of Different Electromagnetic Fields Acts to Reduce the Inflammation in Diabetic Derived Cells. *Int. J. Mol. Sci.* **2023**, *24*, 1754;. https://doi.org/10.3390/ijms24021754.
35. Giuliani, L.; Chistè, O.; Poggi, C.; Mantarrom, M.; Gervino, G.P.; Morando, C. Procedimento e Relativo Dispositivo Basati sull'uso di Campo Elettromagnetico Atti a Contrastare la Diffusione di Virus di Tipo "Corona" in un Organismo (Procedure and Related Device Based on the Use of Electromagnetic Field to Counteract the Spread of Corona-Like Viruses in an Organism). Italian Patent No. 102021000003284, 15 February 2021.
36. Liboff, A.R. The Warburg hypothesis and weak ELF biointeractions. *Electromagn. Biol. Med.*, **2020**, *39*, 45–48. https://doi.org/10.1080/15368378.2020.1737810.
37. Davies, A.M.; Weinberg, U.; Palti, Y. Tumor treating fields: A new frontier in cancer therapy. *Ann N Y Acad Sci*. **2013**, *1291*, 86–95. doi: 10.1111/nyas.12112.
38. Rossi, C.; Foletti, A.; Magnani, A.; Lamponi, A. New perspectives in cell communication: Bioelectromagnetic interactions. *Semin. Cancer Biol.* **2011**, *21*, 207–214. https://doi.org/10.1016/j.semcancer.2011.04.003.
39. Mosmann, T. Rapid colorimetric assay for cellular growth and survival: Application to proliferation and cytotoxicity assays. *J. Immunol. Methods* **1983**, *65*, 55–63. https://doi.org/10.1016/0022-1759(83)90303-4.
40. Donnarumma, G.; Buommino, E.; Baroni, A.; Auricchio, L.; De Filippis, A.; Cozza, V.; Msika, P.; Piccardi, N.; Tufano, M.A. Effects of AV119, a natural sugar from avocado, on Malassezia furfur invasiveness and on the expression of HBD-2 and cytokines in human keratinocytes. *Exp. Dermatol.* **2007**, *16*, 912–919. https://doi.org/10.1111/j.1600-0625.2007.00613.x.
41. Vaiserman, A.M. Hormesis and epigenetics: Is there a link? *Ageing Res. Rev.* **2011**, *10*, 413–421. https://doi.org/10.1016/j.arr.2011.01.004.
42. Kim, S.A.; Lee, Y.M.; Choi, J.Y.; Jacobs, D.R.; Lee, D.H. Evolutionarily adapted hormesis-inducing stressors can be a practical solution to mitigate harmful effects of chronic exposure to low dose chemical mixtures. *Environ. Poll.* **2018**, *233*, 725–734.. https://doi.org/10.1016/j.envpol.2017.10.124.
43. Manni, V.; Lisi, A.; Pozzi, D.; Rieti, S.; Serafino, A.; Giuliani, L.; Grimaldi, S. Effects of ELF 50_Hz Magnetic Field on Morphological and Biochemical Properties of Human Keratinocytes. *Bioelectromag* **2002**, *23*, 298–305. https://doi.org/10.1002/bem.10023.
44. Manni, A.; Lisi, A.; Rieti, S.; Serafino, A.; Ledda, M.; Giuliani, L.; Sacco, D.; D'Emilia, E.; Grimaldi, S. Low Electromagnetic Field (50_Hz) Induces Differentiation on Primary Human Oral Keratinocytes (HOK). *Bioelectromag* **2004**, *25*, 118–126. https://doi.org/10.1002/bem.10158.
45. ICRP. Recommendations of the International Commission on Radiological Protection. *ICRP* **2007**, *37*, 1–332. https://doi.org/10.1016/j.icrp.2007.10.003. Available online: https://www.icrp.org/publication.asp?id=ICRP%20Publication%20103 (accessed on 23 April 2021).
46. Stebbing, T. *A Cybernetic View of Biological Growth—The Maia Hypothesis*; Cambridge University Press: Cambridge, UK, 2011.
47. Hueppe, F.A.T. *The Principles of Bacteriology*; Open Court Publ: Chicago, MI, USA, 1899.
48. Calabrese, E.J. Hormesis: A fundamental concept in biology. *Microb. Cell* **2014**, *1*, 145–149. https://doi.org/10.15698/mic2014.05.145.
49. Calabrese, E.J. Hormetic mechanisms. *Crit. Rev. Toxicol*. **2013**, *43*, 580–606. https://doi.org/10.3109/10408444.2013.808172.
50. Sanders, C.L. Accidents, Test and Incidents. In *Radiation Hormesis and the Linear-No-Threshold Assumption*; Springer: Berlin, Germany, 2010. https://doi.org/10.1007/978-3-642-03720-7.
51. Schmidt, R.F.; Thews, G. *Humann Physiology*, 2nd ed.; Springer: Berlin, Germany, 1989. https://doi.org/10.1007/978-3-642-73831-9.
52. Jeans, J. *Science and Music*. Cambridge University Press: Cambridge, UK, 1937.
53. Devyatkov, N.D. Influence of Millimeter-band Electromagnetic Radiation on Biological Objects. *Sov. Phys. Uspekhi* **1974**, *16*, 568–569. https://doi.org/10.1070/pu1974v016n04abeh005308.
54. Burda, H.; Begall, S.; Cervený, J.; Neef, J.; Nemec, P. Extremely low-frequency electromagnetic fields disrupt magnetic alignment of ruminants. *PNAS* **2009**, *106*, 5708–5713. https://doi.org/10.1073/pnas.0811194106.
55. Ho, M.W.; Popp, F.A.; Warnke, U. *Bioelectrodynamics and Biocommunication*; World Scientific: Singapore, 1994. https://doi.org/10.1142/2267.
56. Lai, H. Exposure to Static and Extremely-Low Frequency Electromagnetic Fields and Cellular Free Radicals. *Electromagn. Biol. Med.* **2019**, *38*, 231–248. https://doi.org/10.1080/15368378.2019.1656645.
57. Barnes, F.; Greenenbaum, B. Some Effects of Weak Magnetic Fields on Biological Systems: RF fields can change radical concentrations and cancer cell growth rates. *IEEE Power Electron. Mag* **2016**, *3*, 60–68. https://doi.org/10.1109/MPEL.2015.2508699.
58. Bersani, F. *Electricity and Magnetism in Biology and Medicine*; Kluwer Academic: New York, NY, USA, 1999.
59. Marino, A.A. *Modern Bioelectricity*; Dekker Inc.: New York, NY, USA, 1988.
60. Batchelor, S.N.; Kay, C.W.M.; McLauchlan, K.A.; Shkrob, I.A. Time-resolved and modulation methods in the study of the effects of magnetic fields on the yields of free-radical reactions. *J. Phys. Chem.* **1993**, *97*, 13250–13258. https://doi.org/10.1021/j100152a032.

61. Pazur, A.K.H.; Schimek, C.; Galland, P. Magnetoreception in microorganisms and fungi. *Open Life Scie*. **2007**, *2*, 597–659. https://doi.org/10.2478/s11535-007-0032-z.
62. Stebbing, A.R.D. Hormesis--the stimulation of growth by low levels of inhibitors. *Sci. Total. Environ.* **1982**, *22*, 213–234. https://doi.org/10.1016/0048-9697(82)90066-3.
63. Pazur, A.K.H.; Scheer, H. The Growth of Freshwater Green Algae in Weak Alternating Magnetic Fields of 7.8 Hz Frequency. *Zeitschrift für Naturforschung C* **1992**, *47*, 690–694. https://doi.org/10.1515/znc-1992-9-1009.
64. Galland, P.; Pazur, A.K.H. Magnetoreception in plants. *J. Plant Res.* **2005**, *118*, 371–389. https://doi.org/10.1007/s10265-005-0246-y.
65. Pazur, A.K.H.; Rassadina, V. Transient effect of weak electromagnetic fields on calcium ion concentration in Arabidopsis thaliana. *BMC Plant Biol*. **2009**, *9*, 47. https://doi.org/10.1186/1471-2229-9-47.
66. Pazur, A.K.H. Calcium ion cyclotron resonance in dissipative water structures. *Electromag. Biol. Med.* **2018**, *37*, 100–113. https://doi.org/10.1080/15368378.2018.1434789.
67. Preparata, G. *QED Coherence in Matter*; World Scientific: Singapore, 1995. https://doi.org/10.1142/2738.
68. Arani, R.; Bono, I.; Del Giudice, E.; Preparata, G. QED coherence and the thermodynamics of water. *Int. J. Mod. Phys. B* **1995**, *9*, 1813–1841. https://doi.org/10.1142/S0217979295000744.
69. Garbelli, A. Proprietà termodinamiche e dielettriche dell'acqua alla luce della teoria complessa delle interazioni molecolari elettrodinamiche ed elettrostatiche (Thermodynamic and dielectric properties of water in the light of the complex theory of electrodinamic and electrostatic molecular interactions). Ph.D. Thesis, University of Milan, Milano, Italy, 2000.
70. Binhi, V.N.; Rubin, A.B. Magnetobiology: The kT paradox and possible solutions. *Electromagn. Biol. Med*. **2007**, *26*, 45–62. https://doi.org/10.1080/15368370701205677.
71. Del Giudice, E.; Giuliani, L. Coherence in water and the kt problem in living matter. In *Thermal Effects and Mechanisms of Interaction between Electromagnetic Fields and Living Matter*; Giuliani, L., Soffritti, M., Eds.; National Institute for the Study and Control of Cancer and Environmental Diseases "Bernardo Ramazzini Institute": Bologna, Italy, 2010; pp. 7–23.
72. Kaiser, F. External signals and internal oscillation dynamics: Biophysical aspects and modelling approaches for interactions of weak electromagnetic fields at the cellular level. *Bioelectrochem. Bioenerg*. **1996**, *41*, 3–18. https://doi.org/10.1016/0302-4598(96)05085-4.
73. De Ninno, A.; De Francesco, M. ATR-FTIR study of the isosbestic point in water solution of electrolytes. *Chem. Phys.* **2018**, *513*, 266–272. https://doi.org/10.1016/j.chemphys.2018.08.018.
74. Huang, C.; Wikfeldt, K.T.; Tokushima, T.; Nordlund, D.; Harada, Y.; Bergmann, U.; Niebuhr, M.; Weiss, T.M.; Horikawa, Y.; Leetmaa, M.; et al. The inhomogeneous structure of water at ambient conditions. *PNAS* **2009**, *106*, 15214–15218. https://doi.org/10.1073/pnas.0904743106.
75. Marchettini, N.; Del Giudice, E.; Voeikov, V.; Tiezzi, E. Water: A medium where dissipative structures are produced by a coherent dynamics. *J. Theor. Biol*. **2010**, *265*, 511–516. https://doi.org/10.1016/j.jtbi.2010.05.021.
76. Montagnier, L.; Aıssa, J.; Del Giudice, E.; Lavallee, C.; Tedeschi, A.; Vitiello, G. DNA waves and water. *J. Phys. Conf. Ser*. **2011**, *306*, 012007. https://doi.org/10.1088/1742-6596/306/1/012007.
77. Smith, C.W. Electromagnetic and magnetic vector potential bio-information and water. In *Ultra High Dilution: Physiology and Physics*; Endler, P.C., Schulte, J., Eds.; Kluwer Academic: Dordrecht, The Netherlands, 1994; pp. 187–201.

Disclaimer/Publisher's Note: The statements, opinions and data contained in all publications are solely those of the individual author(s) and contributor(s) and not of MDPI and/or the editor(s). MDPI and/or the editor(s) disclaim responsibility for any injury to people or property resulting from any ideas, methods, instructions or products referred to in the content.